ISSN 0145-8752, Moscow University Geology Bulletin, 2011, Vol. 66, No. 6, pp. 393–403. © Allerton Press, Inc., 2011.
Original Russian Text © R.R. Gabdullin, A.V. Ivanov, E.A. Shcherbinina, O.V. Zerkal', E.N. Samarin, A.A. Gatina, G.K. Kozlova, E.A. Koshkina, D.V. Nadezhkin, 2011, published in Vestnik Moskovskogo Universiteta. Geologiya, 2011, No. 6, pp. 18–27.

Sequence-Stratigraphic Analysis of the Aptian Deposits in the Valley of the Mzymta River

R. R. Gabdullin[a], A. V. Ivanov[b], E. A. Shcherbinina[a], O. V. Zerkal'[a], E. N. Samarin[a], A. A. Gatina[a], G. K. Kozlova[a], E. A. Koshkina[a], and D. V. Nadezhkin[a]

[a] *Faculty of Geology, Moscow State University, Moscow, 119899 Russia*
e-mail: mosgorsun@rambler.ru
[b] *Saratov State Technical University, Polytechnicheskaya ul., 77, Saratov, 410054 Russia*

Received April 28, 2011

Abstract—In this work, based on the example of a well drilled in the valley of the Mzymta River (Northwest Caucasus) the possibilities of the sequence-stratigraphic method are demonstrated for the first time. This method allows us to clarify the natures of numerous repetitions in the same interval of the geological sequence (modern, ancient landslide or syn-sedimentary-landslide, and tectonic or eustatic). In addition, the geochemical characteristics of bituminous sediments are given. The sequence that was studied in the well shows the complex polygenetic evolution of sediments since Aptian time and the oceanic anoxic event-1.

DOI: 10.3103/S0145875211060056

INTRODUCTION

The sequence-stratigraphic approach allows us to upgrade the literature data, to determine levels of distribution of strong and low-strength rocks, to predict areas of the development of karst cavities and the potential failure of drilling tools, and to optimize the sampling process. In addition, an analysis of the transgressive-regressive (eustatic, or sequent) cycles allows us to divide repeated intervals in the sequence of landslide blocks and variations in sea level accurately, and thus to determine exactly the top of the bedrock massif.

The intense construction of the objects of the Sochi 2014 Olympics in the valley of the Mzymta River has allowed mass development of engineering and geological surveys under the conditions of the very complex geological structure of the region and the development of modern exogenous processes. In this regard, the application of the proposed method is extremely topical.

RESEARCH METHODS

For the first time, based on the example of the sequence of the Carboniferous deposits within the Moscow syncline (an area of the Bersenevskaya embankment, Moscow) it was established that engineering-geological elements (EGE) and sequent systems tracts are in good agreement. As a result of these works, six sequences were selected. In the East European Platform (the area of distribution of the Phanerozoic epicontinental seas) only two systems have been established, as a rule: TST, the transgressive tract system and THS, the highstand tract system (Gabdullin, 2010; Gabdullin and Ivanov, 2010).

The dependence that was established between tract systems and EGE based on the example of a structure with a relatively simple geological structure (the Moscow syncline) was tested in an area with a more complex geological structure, the Northwest Caucasus (Abkhazo-Rachinskaya zone, the Mzymta River valley, the area of the settlement of Kepsha).

In the future, it may be possible to trace single EGE using the regional and transcontinental high-accuracy correlation with methods of event, paleomagnetic, sequence, and cyclic stratigraphy (Gabdullin, 2011). The general principles of the sequence-stratigraphic analysis, particularly for engineering-geological surveys, are given in some works (Gabdullin, Kopaevich, and Ivanov, 2008; Gabdullin et al., 2010).

Application of Sequence-Stratigraphic Analysis for Sections in the Mzymta River Valley.

During engineering-geological surveys in the Northwest Caucasus researchers have to deal with complex structural and tectonic structure of work areas; many modern or ancient landslides occur along ancient faults and thrusts. Due to this, it is difficult to make stratigraphic divisions of sediments. To overcome these difficulties, the methods of applied stratigraphy are used.

This work is based on the results of field works that were carried out in the summer of 2009 within the Kepsha site (Figs. 1a, 1b), which included: (1) five geological routes and 386 points of observation, (2) description of the cores from 86 wells; (3) description of the sections of ten test pits, (4) collection of more than 200 samples of sedimentary rocks from both natural and artificial outcrops, as well as the core, (5) petrographic study of rocks in 115 thin sections according

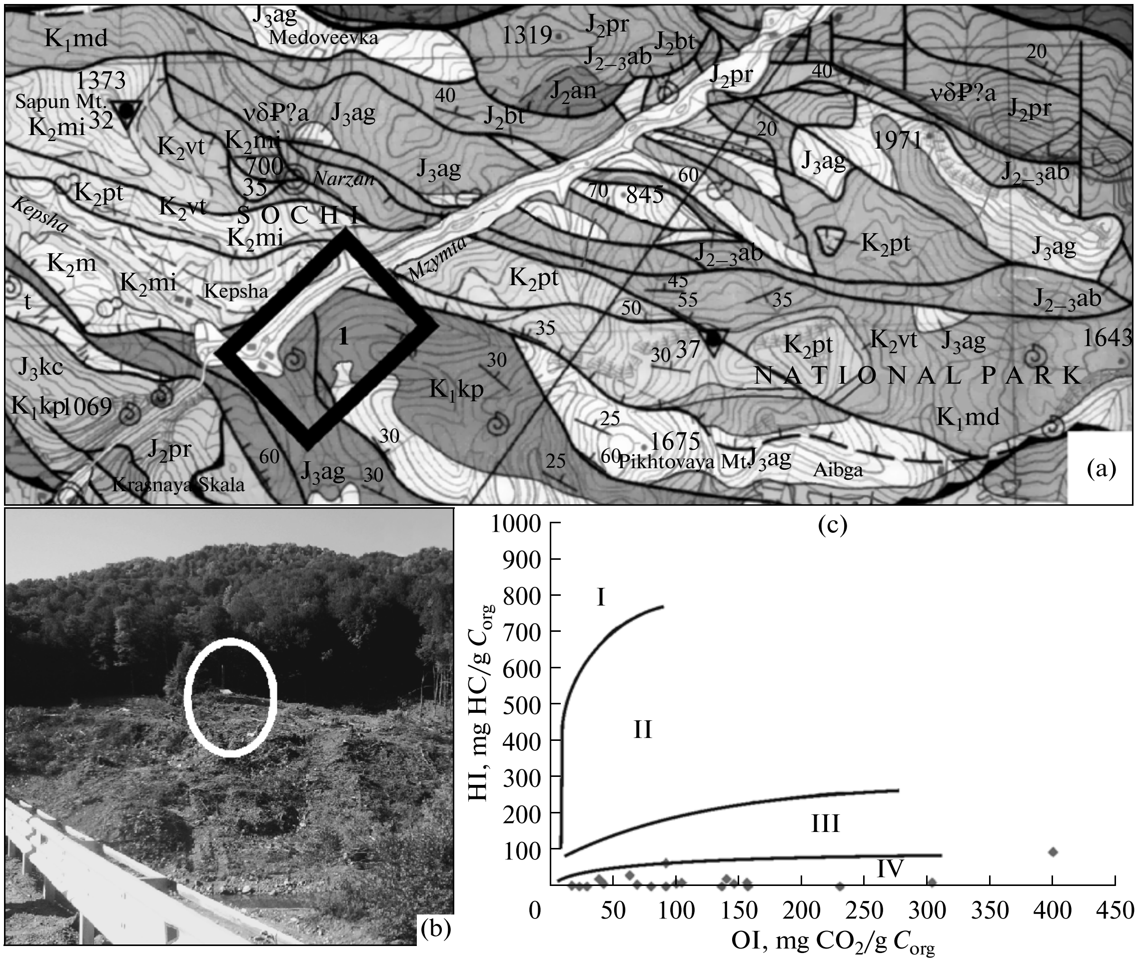

Fig. 1. The scheme of the Kepsha area location:
(a) a fragment of the State Geological Map at the 1 : 50000 scale, (b) the position of well no 568 on the landslide slope on the left bank of the Kepsha River, (c) the results of the pyrolysis according to the Rock-Eval method on a modified Van Krevelen's diagram (HI-OI dependence graph).

to the modified classification by S.G. Vishnyakov, (Shvanov et al., 1998), (6) micropaleontological analysis: identification of Mesozoic radiolarians in 115 thin sections (V.S. Vishnevskaya, Geological Institute of the Russian Academy of Sciences, or briefly GIN RAS), the determination of the Mesozoic foraminifera in the 115 thin sections (L.F. Kopaevich, Moscow State University, or briefly MSU), the definition of the Mesozoic nanoplankton in 200 samples (E.A. Scherbinina, GIN RAS), the determination of the Mesozoic ostracods in 10 samples (E.A. Tesakova, MSU); the age dating of rocks was based on the study of the nanoplankton complex, which can be easily determined in the samples. Ostracods, radiolaria and foraminifera were not found;

(7) macropaleontological analysis: identification of bivalves and cephalopods (E.Yu. Baraboshkin, MSU); (8) geochemical analysis of elements and oxides in 85 samples using a MARC.GV X-ray-fluorescent spectroscope (Spectron NGO, St. Petersburg, analyst E.N. Samarin (MSU)); and (9) the Rock Eval 6 pyrolysis (analyst D.V. Nadezhkin, MSU).

The main difficulties in the division and correlation of geological sections are the follows:

Table 1. Comparative characteristics of lithotypes based on field and petrological descriptions and results of geochemical analysis

No.	Result data of field description	Result data of petrographic description	Result data of geochemical analysis
1	Argillite	Argillite	Calcareous clay
2	Limestone	Bioclastic algae limestone	Clay limestone
3	Micritic marl	Micritic marl	the same
4	Micritic marl	the same	Micritic marl
5	Clay marl	″	Clay dolomitic marl

Table 2. Results of geochemical analysis of elements and oxides from seven samples (well no. 568), obtained using MARC.GV (NPO Spektron, St. Petersburg, analyst E.N. Samarin (MSU))

Component	Depth, m						
	26.3 1	28.0 2	30.0 3	40.0 4	42.6 5	42.8 6	43.9 7
SiO_2	50.1	48.6	54.5	52.5	45.7	59.1	54.4
TiO_2	0.6	0.6	0.7	0.7	0.5	0.8	0.7
Al_2O_3	16.0	15.3	19.8	20.6	15.9	19.2	20.3
Fe_2O_3	4.1	4.2	5.3	6.0	4.7	5.8	5.5
MnO	0.1	0.2	0.1	0.3	0.2	0.1	0.1
CaO	14.2	15.1	10.1	11.6	15.7	6.8	9.6
MgO	1.9	1.9	2.4	3.1	1.8	2.1	2.7
K_2O	2.2	2.2	2.5	2.5	2.2	2.7	2.6
P_2O_5	0.1	0.1	0.1	0.1	0.1	0.1	0.1
S	0.1	0.1	0.1	0.1	0.1	0.1	0.1
$CaCO_3$	25.3	27.0	18.0	20.7	28.0	12.1	17.1
$MgCO_3$	4.0	4.0	5.0	6.5	3.8	4.4	5.6
$CaCO_3 + MgCO_3$	29.3	30.9	23.0	27.2	31.8	16.5	22.8
name, according to the S.G. Vishnyakov's classification (1998), modified	Clay marl	Clay marl	Calcareous clay	Clay dolomitic marl	Clay marl	Calcareous clay	Calcareous clay

(1) Similar lithological composition of units of different ages (mainly terrigenous, clay-dominated species);

(2) The inability to establish and trace the geological boundaries in natural and artificial outcrops and the core.

To overcome the first problem the mineralogical-petrographic methods of applied stratigraphy have been used. As usual, they are applied in a limited area, in which the same geological processes occurred. The works carried out included petrographic study of thin sections and geochemical analysis of the elements and oxides. The lithological composition allowed us to correct the initial field description of the core (Tables 1, 2).

To solve the second problem the paleontological and sequent methods of applied stratigraphy were used. These methods made it possible to date sediments. The age data obtained made it possible to divide and correlate the sections and to estimate levels of beds in areas where landslide processes occur.

When describing the core it is difficult to make a correct prediction, and sometimes to determine the depth of distribution of untouched bed rocks. The sampling for paleontological analysis allowed us to identify the levels of occurrence of multilayered landslide plates on the basis of findings of microfossils of different ages because of their displacement by gravitational processes. In bedrock, there is no such "confusion" with age datings. Analysis of overturned bedding of a bed (that is, establishment of features of their bottom or top) was carried out based on hieroglyphs (mehanogliphs and biogliphs; that is, ichnofossils).

Sequence (or eustatic) analysis makes it possible to distinguish transgressive-regressive series of beds (regular shoaling or deepening of the basin) from multilayer landslide plates. In case of deepening, the gradual transition from one paleo-depth facies to another is not observed.

Stratigraphy and Geochemical Characteristics

Cretaceous rocks in the area of the settlement of Kepsha are terrigenous carbonate sediments, which show alternation in the section without apparent rhythmic structure. In the area of works, located on the landslide slope of the left bank of the Mzymta river, as well as to the west and southwest, the deposits of Aptian and Albian layers of the Lower Cretaceous, and Senomanian, Santonian and Campanian layers of the Upper Cretaceous were described in natural outcrops and wells. In general, the carbonate content in sediments increases up the section: if clays and silts are dominated in the Aptian sediments, then the Albian-Senomanian part of the section consists mainly of clays and bituminous marls interbedding with limestones and clays. The Santonian–Campanian deposits are represented by marls and limestones.

The lower and middle parts of the slope are made of Lower Aptian rocks. Albian deposits are characteristic of the upper part of the slope, where they were opened in several wells. The Senomanian deposits within the area of works are presented only in landslide bodies; in natural outcrops they were described only in the southwest part, in the valley of the unnamed stream, embedded in the left side of the Mzymta River westward of the site of works. The Aptian-Senomanian deposits contain layers of bituminous marls and argillites, which are oil-bearing rocks that formed as a result of anoxic events under eustatic variations in sea level (OAE-1 and 2).

According to the pyrolysis (Table 3), the content of the C_{org} (TOC, wt %) in Aptian bituminous sediments sampled in the middle reaches of the Mzymta river is 0.25–6.88; in Albian deposits, it is 4.07 and in Senomanian deposits, 5.4–6.41. Our findings are similar to those previously published (Afanasenkov et al., 2007): the C_{org} (TOC, wt %) for the Aptian–Albian unstratified deposits is up to 1.25%; for Senomanian deposits, it is up to 10.2%. The Santonian and Campanian deposits lie to the west of the site of the works.

For comparison, Table 3 shows data for the Lower-Middle Jurassic sediments of the Krasnopolyanskaya zone. The content of C_{org} in argillites of the Middle-Upper Jurassic is 0.5–1%, on average (Afanasenkov, Nikishin, and Obukhov, 2007). The maximum C_{org} content in Lower–Middle Jurassic sediments of the Krasnopolyanskaya zone (0.78%) is noted in black low-strength bituminous schists. The content of mineral carbon (c_{min}) in the Jurassic rocks is low (0.07–1.34%).The maximum value was obtained for graphite gray-black thick-lamelled very low-strength bituminous shists, whose age is the Sinemurian Plinsbah, according to the nanoplankton complex. The sum of the peaks ($S_1 + S_2$) < 0.5 mg HC/g of rock points to the absence of any oil and gas potential in the deposits studied . According to the HI-OI dependence graph (Fig. 1C) all samples (Jurassic and Cretaceous) contain type IV kerogen, which contains mostly decomposed organic matter and has no oil and gas potential. The total content of C_{org} is low and varies from 0.07 to 0.78%. The C_{min} in samples of Cretaceous rocks is 0.25–6.88% where the maximum value was obtained for a sample of Early Aptian bituminous marl.

Due to poor exposure, the contacts between sediments described and overlying and underlying stratigraphic units were studied only in a fragmentary manner. The material collected does not allow us to estimate the continuity of the stratigraphic section correctly, as well as the relationships between various strata that were identified and described during geological surveys at the 1 : 500000, 1 : 200000 and 1 : 25000 scales. Therefore, the stratigraphic description of deposits within the site of works is based on the international stratigraphic scale.

As an example, let us consider the geological model of the section of the well 568 m from the depth of 56.5 (from top to bottom):

(1) Quaternary modern active landslide in the interval of 0.0–26.5 m. Loams, high-plastic, low-plastic, semi-solid and solid. Low-plastic clays and detrital soils with clay filling are rare. The fifth (upper landslide) body in the interval of 0.0–10.0 m is recorded, the fourth, in the interval of 10.0–17.6 m, the third, in the interval of 17.6–20.7 m, the second, in the interval of 20.7–24.4 m, the first (the lower landslide), in the interval of 24.4–26.5 m;

(2) The ancient alluvial terrace of the Mzymta River in the interval of 26.5–27.3 m, represented by pebble soil;

(3) Quaternary modern inactive landslide in the interval of 27.3–39.0 m (Fig. 2A). Low-strength loams and clays, highly weathered marls. The upper (the second) landslide body is in the interval of 27.3–37.2 m and the lower, in the interval of 37.2–39.0 m, are distinguished;

(4) The strata of the highly fractured and weathered marls and low-strength argillites in the interval of 9.0–44.1 m deformed by (mechanically disintegrated) landslides (Fig. 2B);

(5) The strata of bituminous marls, argillites and schists in the interval of 44.1–47.7 m with Early Aptian syn-sedimentary landslides (rotation landslides) (Fig. 2B) with persistent elements of rock bedding;

6) Early Aptian marls, argillites and clays in the interval of 47.7–56.5 m with persistent elements of rock bedding (Fig. 2D).

In the elluvial deposits and landslide blocks near the well numerous inoceramus shells *Aucellina* sp. ($K_1al_2^{[1]}$–K_2cm) were found.

Let us analyze the layer-by-layer description of well no. 568, which is located in the drilling area.

Layer 1. The interval of 0.0-9.40 m. The thickness is 9.4m. Brownish-gray semi-solid loam with inclusions of marl gravel (up to 25% of total volume), average strength, from 50 to 100 mm, from the depth of 2.3 m, low-plastic, from 3.4 m, close to high-plastic (up to 15%), decompressed. In the interval of 8.0–9.0 m water seepage is found.

Layer 2. The interval of 9.40–10.0 m. The thickness is 0.6 m. Brownish-gray detrital loam, high-plastic, argillite gravel (from 50 to 80 mm), low strength.

Layer 3. The interval of 10.0–13.90 m. The thickness is 3.9 m. Brownish-gray semisolid loam with inclusions of low-strength gravel (up to 10% of total volume, size of 30–50 mm), interbeds of large gravel of medium strength, with loam filling, water-saturated from the depth of 12.7 m.

Layer 4. The interval of 13.90–16.40 m. The thickness is 2.5 m.

Gray solid loam with inclusion of low-strength argillite gravel (up to 10% of total volume, up to 100 mm) and landwaste (up to 20%).

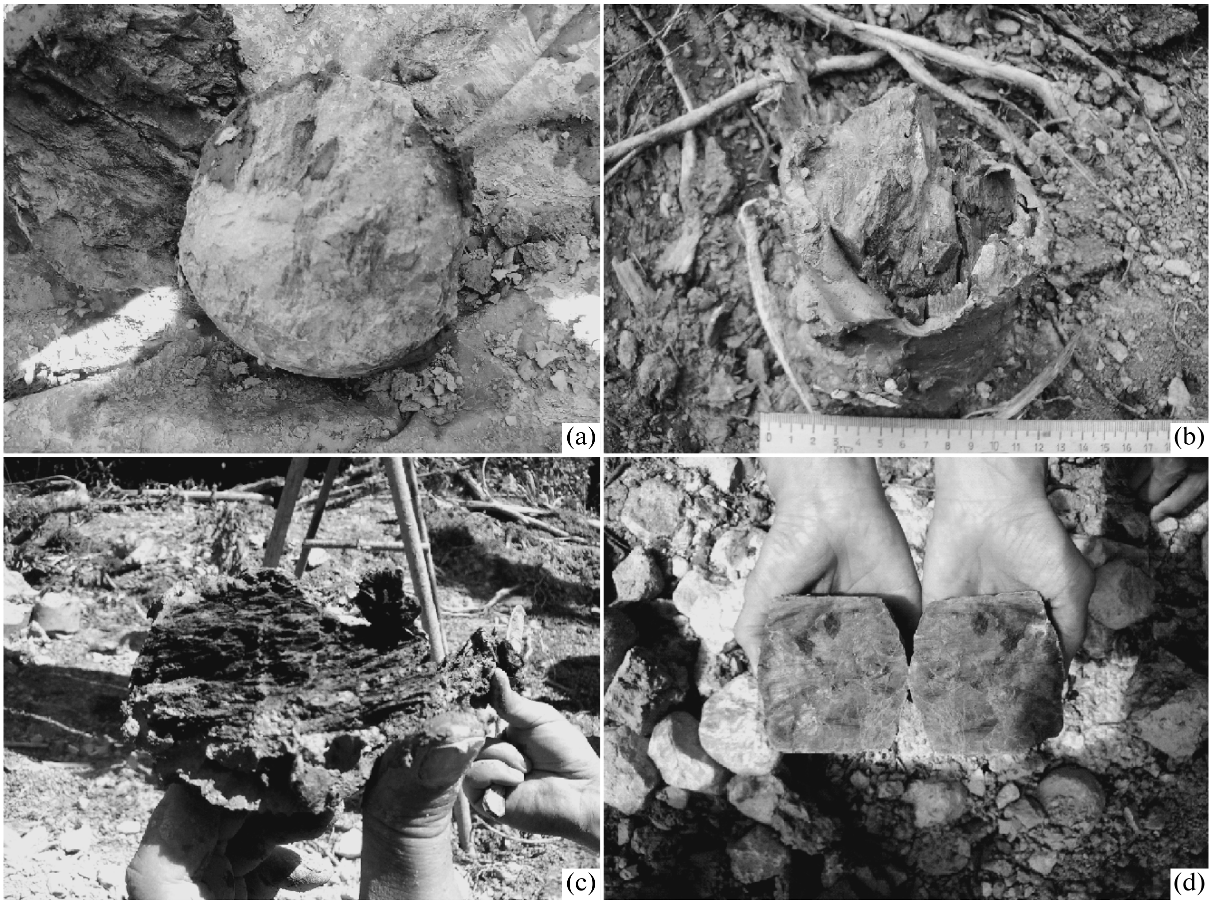

Fig. 2. Images of the core and fossils from the section of the well no. 568.

(a) Dense lens-shaped argillites and loams with gravel-an ancient landslide; (b) the strata of rocks deformed by landslides—brecciaed clay marl gravel; (c) the strata of bituminous marls, argillites and clays (OAE-1) with syn-sedimentary landslides of the Late Aptian. Repeated three times, fan-like bedding, underwater landslides; (d) bituminous marls, argillites and clays of the Late Aptian (OAE-1, the depth of 51.7 m).

Layer 5. The interval of 16.40–17.60 m. The thickness is 1.2 m. A low-plastic pale brown detrital loam with inclusions of gravel and wasteland (up to 60 mm in size; up to 15%) and low-strength argillite blocks.

Layer 6. The interval of 17.60–18.30 m. The thickness is 0.7 m. Dark gray semi-solid loam with inclusions of gravel and landwaste of low strength (up to 30%; size of 20–70 mm), single argillite boulders of medium strength.

Layer 7. The interval of 18.30–20.70 m. The thickness is 2.4 m. Brown low-plastic loam with inclusions of wasteland (up to 15%) and gravel (size of 40 mm) of argillite (up to 10%), as well as single large fragments (more then 140 mm), from the depth of 19.4 m, low-plastic, folded with flattened gravel.

Layer 8. The interval of 20.70–21.40 m. The thickness is 0.7 m. Gray low-plastic clay with inclusions of landwaste (10%) and gravel (15%) of low strength (up to 70 mm in size).

Layer 9. The interval of 21.40–23.20 m. The thickness is 1.8 m. Detrital soil with loam filling (30%), pale brown, an average degree of water saturation, low-plastic filling. Gravel is large, low strength, flattened.

Layer 10. The interval of 23.20–25.20 m. The thickness is 2 m. Pale brown detrital loam, low-plastic, interbedded with high-plastic loams, in the interval of 24.1–24.4 m, low strength water-saturated gravel.

Layer 11. The interval of 25.20–25.80 m. The thickness is 0.6 m. Pale gray detrital loam with inclusions of argillite gravel (up to 10%), low-plastic.

Layer 12. The interval of 25.80–26.50 m. The thickness is 0.7 m. Gray clay with gravel (up to 15%), folded, at the depth of 26.2 m (at an angle of 60–70°), contact with dark gray clays.

Layer 13. The interval of 26.50–27.30. A thickness of 0.8 m. Brown pebble soil with loam filling (up to 15%), with boulders (up to 10%), water-saturated.

Layer 14. The interval of 27.30–28.50 m. The thickness is 1.2 m. Brownish-gray low-plastic argillite,

Table 3. Geochemical characteristic of Jurassic and Cretaceous sediments enriched in organic matter, according to the data of Rock Eval 6 pyrolysis, analyst D.V. Nadezhkin (MSU)

Number of sample	Age of rocks	Lithology	S_1	S_2	PI	T_{max}	S_3	PC	RC	C_{org}	HI	OI	C_{min}
			Free HC to 300°C, mg HC/g rock	HC-products of the kerogen pyrolysis and resins and asphaltine components, 300–600°C, mg HC/g rock	Productivity index, S1/(S1 + S2)	Temperature of maximum HC output at the kerogen pyrolysis, °C	CO_2 content, released during kerogen pyrolysis, mg CO_2/g rock	Pirolised organic carbon, wt %	Residual (non-pirolused) organic carbon, wt %	Total content of organic carbon in rock, wt %	Hydrogen index, mg HC/g C_{org}	Oxygen index, mg CO_2/g C_{org}	Content of mineral carbon in rock, wt %
2k/09	K_1a	Bituminous marls	0.01	0	0.84	–	0.38	0.02	0.26	0.28	0	136	0.25
453/1	K_1a	″	0.01	0.01	0.47	–	0.13	0.01	0.12	0.13	8	100	2.37
453/3	K_1a	″	0.01	0.01	0.47	–	0.19	0.01	0.12	0.13	8	146	2.2
454/5	K_1a	″	0.01	0.23	0.05	441	0.49	0.04	0.74	0.78	29	63	2.7
454/6	K_1a	″	0	0.05	0.06	–	0.47	0.02	0.43	0.45	11	104	4.2
469/1	K_1a	Sandy marls	0	0	1	–	0.11	0.01	0.06	0.07	0	157	5
470/3	K_2s	Bituminous marls	0.04	0.38	0.1	438	0.55	0.06	0.54	0.6	63	92	5.4
492/1	K_2s	″	0.01	0.13	0.08	–	0.56	0.03	0.11	0.14	93	400	6.41
495A	K_1al	″	0.01	0.09	0.12	–	0.17	0.02	0.43	0.45	20	38	4.07
568/42.5	K_1al	″	0.01	0.02	0.39	–	0.11	0.01	0.25	0.26	8	42	2.96
684/3a	K_2s	″	0.01	0.02	0.34	–	0.7	0.03	0.2	0.23	9	304	3.24
728/4	K_1a_1	″	0.01	0.01	0.58	–	0.14	0.01	0.08	0.09	11	156	6.88
458/1	J	Argillites	0	0	1	–	0.76	0.02	0.31	0.33	0	230	0.08
460/3	J_1p–t	″	0.01	0	1	–	0.14	0.01	0.47	0.48	0	29	0.25
460/6	J_1p–t	″	0	0	1	–	0.22	0.01	0.23	0.24	0	92	0.08
460/8	J_1p–t	″	0.01	0.03	0.22	–	0.21	0.01	0.14	0.15	20	140	0.07
461/1	J_2b	″	0.01	0	1	–	0.11	0.01	0.37	0.38	0	29	0.26
462/1	J_2a	″	0.01	0.03	0.3	–	0.54	0.03	0.75	0.78	4	69	0.32
463/1	J_2a	″	0.01	0	1	–	0.36	0.01	0.44	0.45	0	80	0.19
464/1	J_1p–t	″	0.02	0.02	0.59	–	0.1	0.01	0.59	0.6	3	17	1.34
465/1	J_1p–t	″	0.01	0	1	–	0.15	0.01	0.64	0.65	0	23	0.29

weathered, highly fractured, the core recovery is 20% as 6–7 cm core semi-cylinders, 40% as small fragments, and 40% as sludge.

Layer 15. The interval of 28.50–29.30 m. Thickness of 0.8 m. Pale gray detrital loam, with inclusions of argillite gravel (up to 10%), low-plastic.

Layer 16. The interval of 29.30–33.20 m. A thickness of 3.9 m. Brown low-strength argillite, weathered, highly fractured, the core recovery is 10% as debris with a size of 6–7 cm. Fractures are oriented mainly at an angle of 60–70°, vertical fractures are partially clay-filled. From the depth of 31.2 m argillite is water-saturated.

According to the study of thin sections, from the depth of 29.3 m (Figs. 3A, 3B)—micritic marl, not bedded, highly clayed (30%), with lenses and spots of organic matter (20%), with admixture of fine-grained and aleurolitic non-rounded and subrounded calcite and quartz grains(5%), with rare silty mica, intensively gypsified (10%); 45% of carbonates. There are a large number of fractures of different orientations of up to 0.04 in thickness, incrusted by micritic calcite. In addition there are pores with a size of 1 mm, extended in one direction and surrounded by micritic calcite.

Layer 17. The interval of 33.20–33.90 m. The thickness is 0.7 m. Dark gray low-plastic loam with inclusion of argillite landwaste (~5%) and gravel (up to 10%), interbedded with low strength marl and argillite.

Layer 18. The interval of 33.90–34.60 m. The thickness is 0.7 m. Brown low-strength marl, highly fractured, the boundary with an overlying layer is at an angle of 60°, water-saturated.

Layer 19. The interval of 34.60–37.20 m. The thickness is 2.6 m. Pale gray low-plastic clay with flattened argillite fragments with slipping planes; the content of fragments is up to 10%. Throughout a layer interbeds of low strength argillite weathered to low-plastic clay, with inclusions of gravel are traced. The thickness of layers is 10–15 cm. At the base of a layer is a slipping plane along an argillite interlayer.

Layer 20. The interval of 37.20–39.00 m. The thickness is 1.8 m. Pale gray low-plastic clay with flattened argillite fragments with slipping planes; the content of fragments of very low-strength argillite is up to 10%.

Layer 21. The interval of 39.00–40.60 m. The thickness is 1.6 m. Gray low-plastic marl, weathered, highly fractured, interbedded with very low-strength marls, weathered to a state of gravel, with clay filling.

According to the study of thin sections, at the depth of 40.0 m (Figs. 3C, 3D) are clay dolomitic marl; clay limestone (micritic, polymictic, laminated) (20%) with the remnants of foraminifera shells and undetermined detritus (10%); dolomitic limestone (10–15%) with interclasts of organic matter as microlenses and microdroplets (3–9%), with large bioclasts of regenerated crinoids, low gypsified (5%); 45% carbonates. Secondary changes are represented by iron oxides.

Layer 22. The interval of 40.60–42.00 m. The thickness is 1.4 m.

Gray argillite, highly weathered to the state of gravel, with clay filling (up to 40%), low-strength gravel.

Layer 23. The interval of 42.00–44.10 m. The thickness is 2.1 m. Dark gray average-strength argillite with interbeds of low-strength argillite, fractured; fractures are vertical.

According to the study of thin sections, at the depth of 42.5 m (Figs. 3E, 3F) are clay marl (15–20%) with foraminifera (10–20%), undetermined shell detritus. Thin and horizontal layers are due to microlenses and microdroplets of organic matter. Poorly dolomitic with single grains of quartz. In the rock the following nanoplankton complex was described: *Watznaueria barnesae*, *Rotelapillus Iafflttei*, *Biscutum constans*, *Zeugrhabdotus embergerii*, *Z. diplogrammus*, *Micrantolithus hoschulzii*, *Nannoconus* sp., *Rhagodisus asper*, *Flabellites oblongus*, *Micrantolithus obtusus*, *Manivitella pemmatoidea*.

Layer 24. The interval of 44.10–47.70 m. The thickness is 3.6 m. Interbedding of brownish-gray, low strength, weathered marls with those, weathered to gray low-plastic clay, calcification pockets. A thickness of 3–5 cm. Towards the base of a layer the thickness of sub-layers decreases to 1–3 cm. Boundaries of sublayers are oriented at an angle of 60–70°. Marl is sub-vertical-bedded.

Layer 25. The interval of 47.70–56.50 m. The thickness is more than 8.8 m. Interbedding of brownish-gray, low-strength, weathered marls with those, weathered to gray semi-solid, dense clay, calcification pockets. A thickness of 3–5 cm. In the depth interval of 49.0–49.5 m marl is fractured, low-strength; in the interval of 51.5–51.7 m, marl is of average strength, water saturated. The boundaries between layers are at an angle of 60–70°.

At the depth of 49.2 m (Figs. 3G, 3H) is micritic laminated marl with an admixture of quartz grains (20%) and organic matter (about 10%), gypsified. The bulk of the rock is made of carbonate material (60%). The secondary changes are iron oxides.

According to the study of thin sections, at the depth of 56.5 m (Figs. 3I, 3K) are micritic marl, non-bedded with a low admixture of fine-dispersed clay component (5%), with undetermined shell detritus (15%) and single foraminifera shells, with admixture of non-rounded silty quartz. The content of organic matter is 5–7%. The bulk of the rock is made of carbonate material (70%). The next nanoplankton complex was described: *Watznaueria barnesae*, *Rotelapillus laffittei*, *Biscutum constans*, *Zeugrhabdotus embergerii*, *Z. diplogrammus*, *Hayesites irregularis*, *Micrantholithus obtustus*. This complex corresponds the Early Aptian zone of NC6 and allows us to suggest the Early Aptian age of this formation.

It should be noted that the clayey silt layers between thin interlayers of clay marls and micritic limestones can be of several meters in thickness.

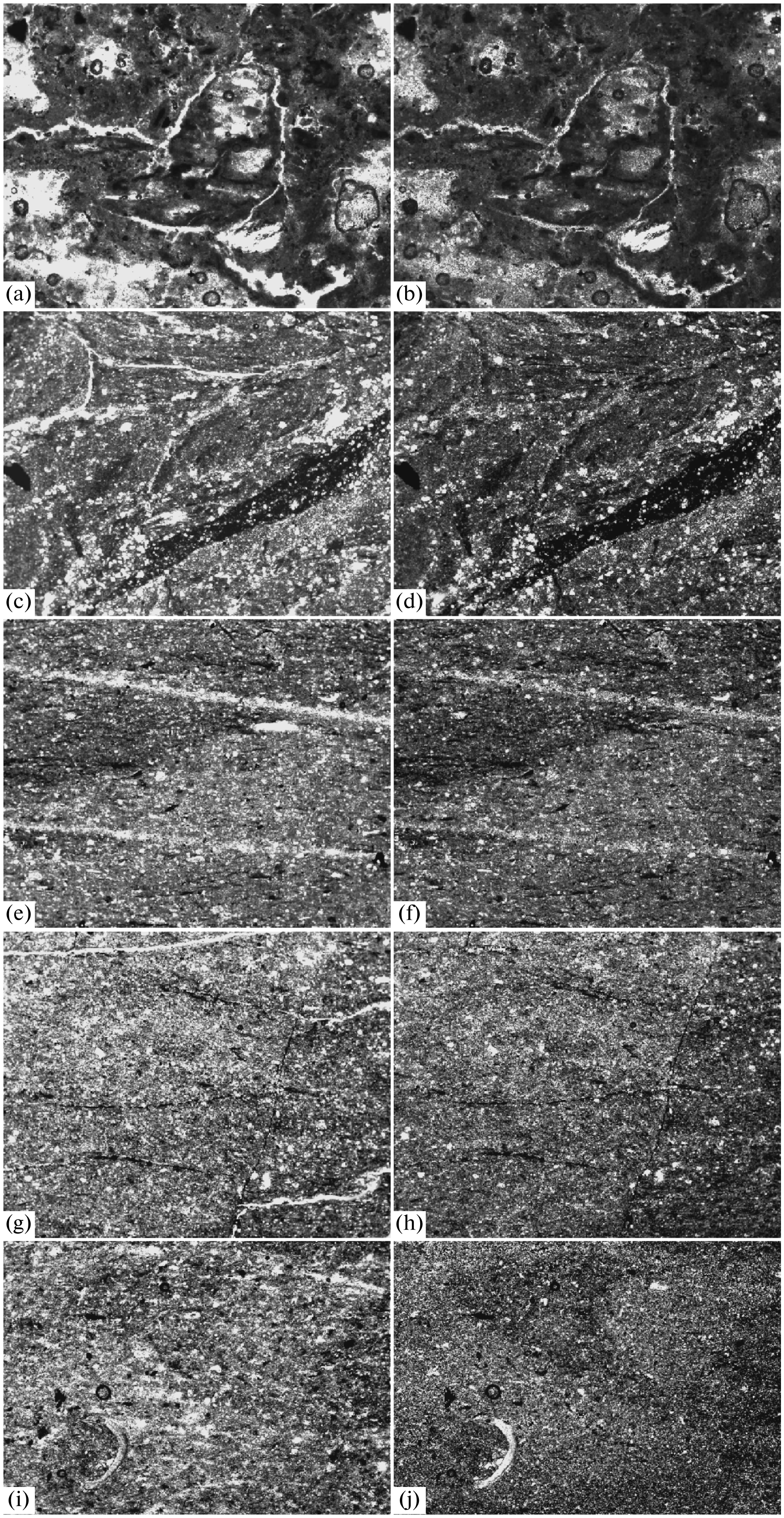
(a)
(b)
(c)
(d)
(e)
(f)
(g)
(h)
(i)
(j)

Fig. 3. Microphotographs of thin sections of the core from the well no 568. (a) The thin section 568, the depth of 29.3 m; (b) the same with crossed nicols; (c) the thin section 568, the depth of 40.0 m; (d) the same with crossed nicols; (e) thin section 568, the depth of 42.5 m; (f) the same with crossed nicols; (g) the thin section 568, the depth of 49.2 m; (h) the same with crossed nicols; (i) the thin section 568, the depth of 56.3 m; (j) the same with crossed nicols.

The contact between Lower Aptian sediments and the underlying rocks is not determined. The sediments described are overlaid with an unconformity by terrigenous–carbonate formations of the Upper Aptian-Lower Albian.

At the depth of at 23.1–23.3 meters the next nanoplankton complex was described: *Watznaueria barnesae*, *W. Z. diplogrammus*, *Rhagodisus asper*, *R. angustus*, *Eprolithus floralis*, *Flabellites oblongus*.

The appearance of *Eprolitus floralis* allows us to refer surrounding sediments to the Upper Aptian zone NC7.

At the depth of 32.3–32.5 m in clayed marls Early Aptian nanoplankton complex was described:

Watznaueria barnesae, *Rotelapillus laffittei*, *Biscutum constans*, *Zeugrhabdotus embergerii*, *Z. diplogrammus*, *Micrantolithus hoschulzii*, *Nannoconus* sp., *Rhagodisus asper*, *Flabellites oblongus*, *Micrantholithus obtustus*, *Manivitella pemmatoidea*.

However, the upper 44.1 m interval of the well section is across a landslide body. Consequently, it is evident that the boundary between sediments of the lower and upper sub-stages of the Aptian stage lies higher up the slope. Below this interval nanofossils were selected from bedrock fragments in the landslide bodies. Only from this depth sedimentary rocks with the persistent elements of bedding and textural and structural features typical of the bedrocks (bedding, bioturbation, and underwater landslides at the top of the sequence, etc.) are noted.

According to the stratigraphic volume, the deposits described correspond to the Kepsha suite (K_1 *kp*), which is the age analogue of the Medoveevskaya suite. The Kepsha suite occurs in the southern subzone of the Chvizhepse zone, in the core of the Dagomys anticline. It is underlain by deposits of the Agepstinskaya suite.

The overlying deposits of the studied area are unknown. In the area of the settlement of Solokh-Aul the sequence is represented by fukoid greenish-gray marls. In the lower part there are limestone layers (up to 50 cm); in the upper part are horizons of brownish marls (10–15 m) and sub-layers of aleurolites and cherts (1–5 cm). The thickness is more than 380 m. Further east, in the valley of the Mzymta River it is estimated to be 460 m. An Early Cretaceous age of these deposits was determined based on the numerous findings of *Neohibolites minimus* List., *Aptychus exculptus* Schurr., *Berriasella cf. subrichteri* Ret., *Lamellaptychus cf. angulicostafus* Picf et. Lor., *Duvalia lata* Blain and others.

DISCUSSION OF RESULTS

On the basis of field and laboratory (thin sections) description of the section of the well 568, the following geological and genetic model is proposed.

In the unconsolidated Quaternary sediments a series of landslide plates (blocks) was selected. The sleeping planes and sub-layers of low-strength and high-strength loams and clays sometimes with gravel and landwaste of bedrocks (marls, argillites), which alternate with beds of loams and highly weathered solid and semi-solid bedrocks, are considered to be the boundary between individual plates (Fig. 4). The sub-layers of low-strength and high-strength loams and clays, sometimes with gravel and landwaste of the bedrocks, as a rule, overlie the sleeping planes. In case a sleeping plane is not noted in the core (or the core recovery is poor), the base of such layers are conventionally taken as this boundary. The landslide blocks contain displaced fragments of weathered bedrocks of the Aptian age, according to the findings of nanoplankton species, but they are enclosed in sandy loam soils. Often in the core of wells, numerous repetitions in the section can be observed. This is interpreted to be the result of landslides. It is important to distinguish the core interval with repeated elements of the section of the landslide massif from the tectonic repetition of the fragments of the section due to thrusting processes (the research area is characterized by strong tectonic dislocations and deformations) and transgressive–regressive cycles.

The sequence-stratigraphic analysis allows us to identify transgressive (retrograde) three-element (*A*-*C*) series in the bedrocks, repeated three times in the well section. The first element (*A*) is marl, the second (*B*)-calcareous argillite or clay, and the third (*C*) is argillite or clay with calcification pockets. As a result of eustatic variations the cyclic structure of the section with repeating fragments (cycles or cyclites) forms. The latter may have different or the same (actually almost the same) thickness and structure. These differences can be observed in outcrops, but in the core these fragments are difficult to divide. Cyclic variations in sea level are also confirmed by the cyclic occurrence of levels of bituminous sediments in the sequence.

This sequent cyclicity, which resulted from eustatic variations in the level of sedimentation basin, is clearly manifested in the sequence of the massif and is not associated with modern landslide processes. Almost always in the sequence the gradual and mainly regular natural transition from shallow facies to deep water or vice versa is seen.

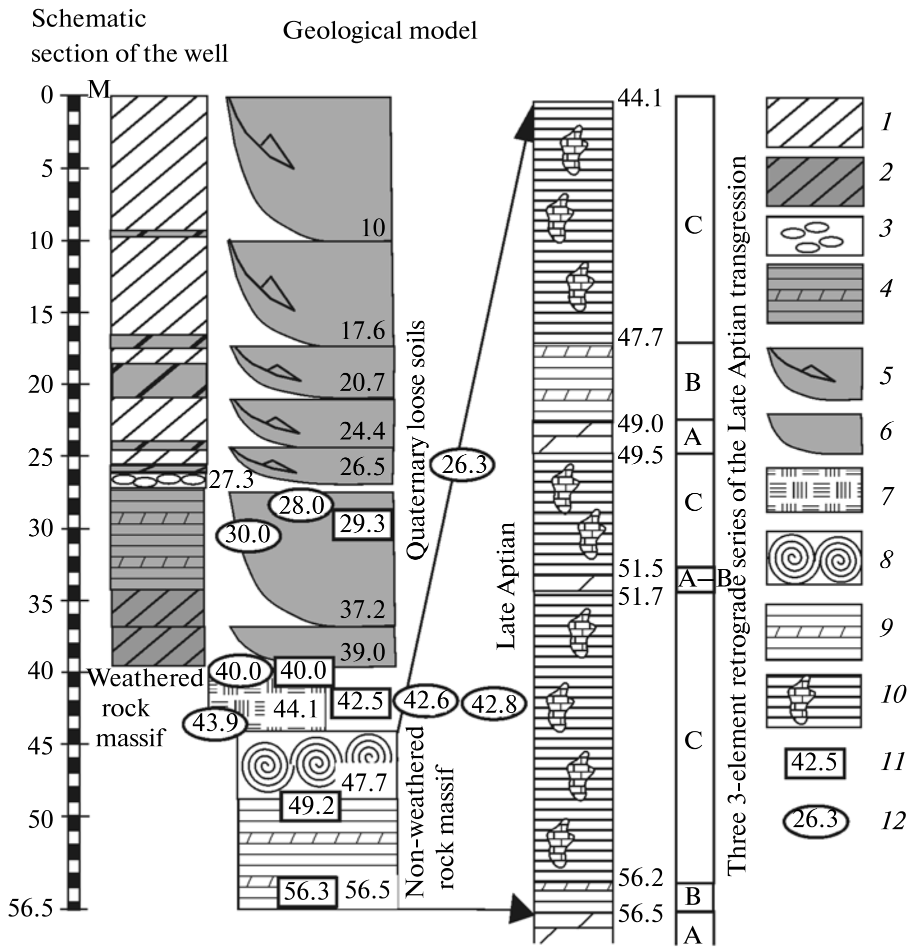

Fig. 4. Schematic section of the well and the geological model. *1*, solid and semi-solid loams; *2*, low-plastic and high-plastic loams; *3*, pebble and gravel-pebble soils of ancient alluvial terraces of the Mzymta River; *4*, highly fractured low-strength argillites and marls, solid and semisolid loams; *5*, active landslide (plate); *6*, inactive landslide (plate); *7*, the strata of rocks deformed by landslides; *8*, strata of bituminous marls, argillites and clays of the Lower Aptian of syn-sedimentary landslides; *9*, marls, argillites and clays of the Late Aptian; *10*, clays and argillites with the centers of carbonation; *11*, a depth of thin sections, m; *12*, depth of sampling for geochemical analysis, m.

In the case of the tectonic juxtaposition of the sequence fragments, the probability of gradual transition is practically close to zero. At landslide processes such probability is higher. Landslide processes in the Aptian time occurred synchronously with the sedimentation, which is clearly recorded by underwater landslides, that is, underwater landslides, which are clearly different from modern landslides and tectonic dislocations.

CONCLUSIONS

1. For the first time in the area of the valley of the Mzymta River, based on the example of well-section study, the sequence-stratigraphic method, which allows one to clarify the nature of numerous repetitions of the same interval in the geological sequence (modern, ancient or syn-sedimentary-landslide, and tectonic or eustatic), was tested.

2. Based on the example of the well section, the complex polygenetic evolution of the sequence was shown.

3. The extensive development of artificial outcrops in the research area, which are temporarily available for geological survey due to the construction of the objects of the Sochi 2014 Olympics, provides a unique opportunity to study the regional and historical geology of the area, as well as oil source rocks that formed during oceanic anoxic events in the Cretaceous (and other) ages for the prediction of the oil and gas potential of the Black Sea–Caspian region.

ACKNOWLEDGMENTS

We thank E.A. Voznesenskii and A.M. Nikishin for critical review of this work.

REFERENCES

Afanasenkov, A.P., Nikishin, A.M., and Obukhov, A.N., *Geologicheskoe stroenie i uglevodorodnyi potentsial Vostochno-Chernomorskogo regiona* (Geological Structure and Oil-and-Gas Potential of the East Black Sea Region), Moscow: Nauka, 2007.

Gabdullin, R.R., Ivanov, A.V., Koshelev, A.V., and Kopaevich, L.F., *Trening po sekventnoi stratigrafii: Ucheb. posobie po povysheniyu kvalifikatsii spetsialistov* (Training on Sequent Stratigraphy: Guidance for Continuing Education), Moscow: Izd-vo Mosk. Univ., 2010.

Gabdullin, R.R., Kopaevich, L.F., and Ivanov, A.V., *Sekventnaya stratigrafiya* (Sequent Stratigraphy), Moscow: Maks-Press, 2008.

Gabdullin, R.R. and Ivanov, A.V., Sequence-Stratigraphic Approach for Engeneering-Geological Works. Problems of Geology, Geoecology and Rational Use of Nature. in *Mat-ly Vseros. nauch. simpoz* (Proc. All-Russian Sci. Conf.), Saratov: Nauka, 2010, pp. 36–37.

Gabdullin, R.R., Sequence-Stratigraphic Approach during Engeneering-Geological Works, *Moscow Univ. Geol. Bull.*, 2010, vol. 65, no. 6, pp. 410–414.

Gabdullin, R.R., A High-precision Planetary Stratigraphic Correlation of Sedimentary Phanerozoic Sequences Using a Combination of Methods of Event, Paleomagnetic, Sequence and Cyclic Stratigraphy, *Moscow Univ. Geol. Bull.*, 2011, vol. 66, no. 1, pp. 21–28.

Shvanov, V.N., Frolov, V.T., Sergeeva, E.I., et al., *Sistematika i klassifikatsii osadochnykh porod i ikh analogov* (Systematics and Classification of Sedimentary Rockas and Their Analogues), St. Petersburg: Nedra, 1998.